

Wavelength switching in InGaAs/InP quantum well lasers

K. Berthold, A. F. J. Levi, T. Tanbun-Ek, and R. A. Logan
AT&T Bell Laboratories, Murray Hill, New Jersey 07974

(Received 5 September 1989; accepted for publication 31 October 1989)

The threshold current density of multiple and single quantum well lasers as a function of cavity length has been investigated. A dramatic change of the lasing wavelength and a strong increase of the threshold current density is observed for a single quantum well laser when the cavity length is reduced to $\sim 400 \mu\text{m}$. In addition, discrete widely separated wavelength switching with changes up to 50 nm is achieved using an intracavity electroabsorption region.

One of the important advantages of quantum well lasers is that optical gain is accessible over a large energy range. This allows the possibility of wavelength tuning and switching involving significant changes in photon energy. In general such tuning may be achieved by varying laser cavity losses. A simple way to do this is to vary the cavity length and thus change the relative contribution of mirror losses. This has been intensively studied for single quantum well (SQW) lasers in the GaAs/AlGaAs material system.¹⁻⁵ However, no such study has been published for SQW lasers in near-infrared materials such as InGaAs/InP. In fact, it is only recently that high performance SQW lasers of InGaAs/InP have been reported.^{6,7}

In this letter we report on the cavity length dependence of the threshold current and lasing wavelength using high quality, graded-index separate confinement (GRINSCH) InGaAs/InP single and multiple quantum well lasers. In addition, we demonstrate a novel technique to electrically switch lasing wavelength using a monolithically integrated electroabsorption region in buried-heterostructure (BH) SQW and multiple quantum well (MQW) lasers.

InGaAsP crystals were grown by atmospheric pressure metalorganic vapor phase epitaxy (MOVPE).⁶ The epitaxial layers were grown on a (100) *n*-InP substrate using the following growth steps. First an *n*-type InP buffer layer 1 μm thick was grown. The lower part of the GRINSCH layers with 22-nm-thick step-like undoped quaternary layers lattice matched to InP with a decreasing band gap of 1.0, 1.1, 1.25, and 1.33 μm for a SQW and 1.0, 1.1, 1.2, and 1.25 μm for a MQW was then grown. A single ternary quantum well of thickness d in the range $14 \text{ nm} < d < 18 \text{ nm}$ for a SQW, or MQWs with $d = 9 \text{ nm}$ cladded by InGaAsP (1.25 μm , 25-nm-thick band-gap wavelength) barriers was grown next. Following this, the upper part of the undoped GRINSCH InGaAsP confining layers analogous to the lower ones but with an increasing band gap from 1.33 to 1.0 μm for the SQW and from 1.25 to 1.0 μm for the MQW was grown. The remainder of the structure consists of an InP setback layer to minimize effects of Zn diffusion from the upper cladding (50 nm thick, undoped), a *p*-InP cladding layer (1–2 μm thick), and a *p*-InGaAsP cap layer.

We systematically investigated the lasing characteristics of broad-area SQW and MQW InGaAs/InP lasers (50 μm stripe width) as a function of cavity length L_c . Starting with $L_c = 2.5 \text{ mm}$, we progressively reduced L_c by cleaving the same sample. Figure 1(a) shows the threshold current

density j_{th} as a function of the cavity length L_c for a SQW ($d \sim 16 \text{ nm}$) and a four QW ($d \sim 9 \text{ nm}$) laser. The threshold current density for the four QW laser increases monotonically from $j_{th} = 450 \text{ A cm}^{-2}$ at $L_c = 2.4 \text{ mm}$ to $j_{th} = 0.9 \text{ kA cm}^{-2}$ at $L_c \sim 500 \mu\text{m}$. However, the threshold current density of the SQW increases from $j_{th} = 750 \text{ A cm}^{-2}$ at $L_c = 2.5 \text{ mm}$ to $j_{th} = 2 \text{ kA cm}^{-2}$ at $L_c \sim 500 \mu\text{m}$ and then abruptly increases to $j_{th} = 6 \text{ kA cm}^{-2}$ for cavity length $L_c < 500 \mu\text{m}$. The corresponding lasing wavelength λ is illustrated in Fig. 1(b) as a function of cavity length. As also may be seen in the figure, the lasing wavelength for the four QW structure decreases only slightly from $\lambda = 1.61$ to $1.58 \mu\text{m}$

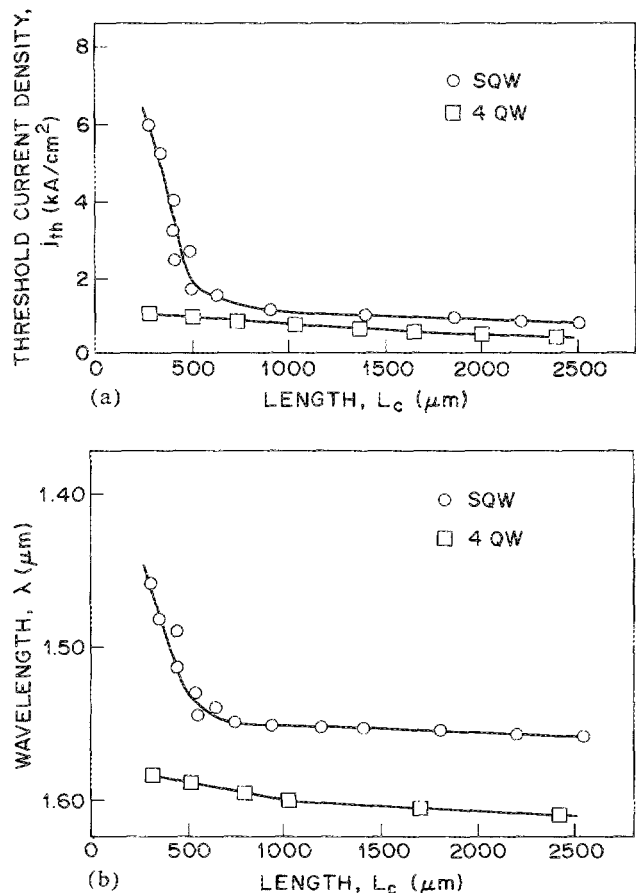


FIG. 1. (a) Threshold current density j_{th} vs cavity length L_c for a SQW ($d \sim 16 \text{ nm}$) and a four QW ($d = 9 \text{ nm}$) GRINSCH broad-area laser. (b) Lasing wavelength λ as a function of cavity length L_c for a SQW ($d = 16 \text{ nm}$) and a four QW ($d = 9 \text{ nm}$) GRINSCH broad-area laser.

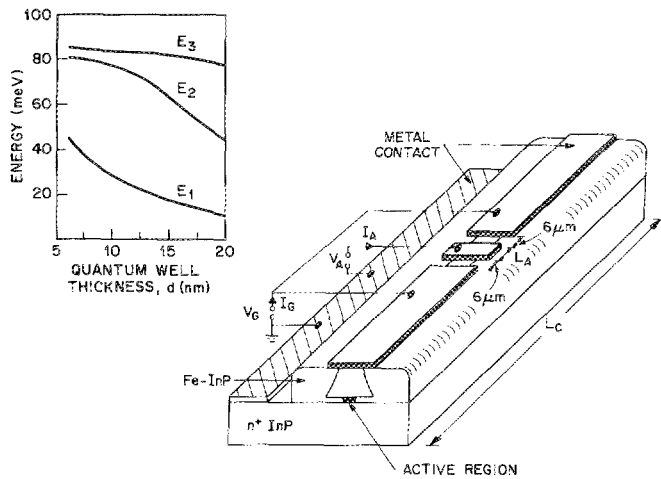


FIG. 2. Schematic sketch of a BH GRINSCH QW laser diode with a cavity length L_C and an absorber length L_A . The gain current I_G into the large segments, the absorber voltage V_A , and the absorber current I_A at the small segment are indicated. The inset shows the calculated electron confinement energies for a GRINSCH QW laser as a function of quantum well thickness d .

for the shortest cavity length. However, for the SQW λ decreases from $\lambda = 1.56$ to $1.46 \mu\text{m}$.

A calculation of the electron confinement energies versus quantum well thickness for the SQW GRINSCH structure with a 40% conduction-band and 60% valence-band offset is presented in the inset in Fig. 2. An effective electron mass of $m_e^* = 0.041m_0^*$ (where m_0^* is the free-electron mass) was used for solving the bound-state energies of the GRINSCH QW potential. The calculations show that λ for the four QW laser is in good agreement with the lowest subband ($n = 1$) heavy hole transition. The measured λ for the SQW lasers is in good agreement with the second subband ($n = 2$) heavy hole transition. For the shortest SQW lasers, λ sharply decreases to $1.46 \mu\text{m}$ by tuning through the $n = 2$ energy level.

Although the threshold current densities for SQW lasers presented in this letter are the lowest reported in the literature,⁶ we have only observed lasing action in SQW diodes from the second quantized state ($n = 2$). Experimentally, lasing occurs at up to 20 meV higher energy than the electroluminescence peak depending on the quantum well width and cavity length. This accounts for the higher threshold current density of SQW compared to MQW lasers. Further lowering of the threshold current density is expected if SQW structures operating at lower loss and $n = 1$ level can be fabricated. For four QW broad-area devices only lasing from the first subband is observed for cleavages $2.5 \text{ mm} > L_C > 200 \mu\text{m}$. When cavity length is reduced to $L_C \approx 100 \mu\text{m}$, lasing from the $n = 2$ level ($\lambda \approx 1.46 \mu\text{m}$) is measured and the threshold current density increases to 6 kA cm^{-2} .

Encouraged by the wavelength dependence of broad-area SQW lasers with varying cavity losses, we fabricated BH SQW and MQW lasers with a monolithically integrated electroabsorption region in order to electrically change the

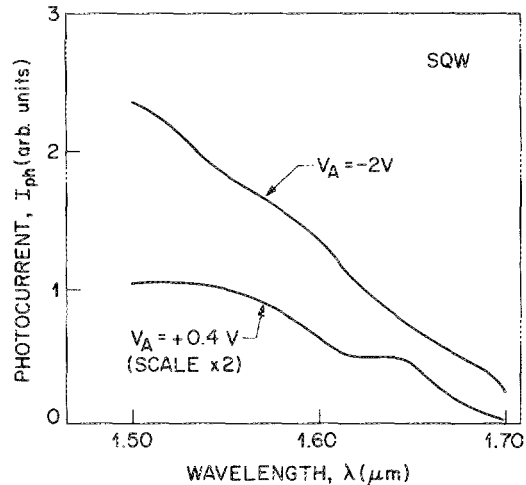


FIG. 3. Photocurrent I_{ph} vs wavelength utilizing TE-polarized light for a SQW ($d = 18 \text{ nm}$) and two different voltages.

internal cavity loss. The BH lasers were fabricated by reducing the width of the active region utilizing a selective etch and a regrowth procedure using Fe-InP and MOVPE as described in Ref. 8. Electrical contacts to the p^+ contact layer are achieved using three photolithographically defined metal stripes as shown in Fig. 3. The gap between the metal stripes is $6 \mu\text{m}$ and the length of the small segment is L_A . After etching off the InGaAsP contact layer in the gap region, the resulting isolation resistance between the segments is $> 3 \text{ k}\Omega$. As illustrated in Fig. 2 the two long metal stripes are electrically connected and defined as the gain region whereas the small section is defined as the modulation absorber region.

A typical photocurrent spectrum for a GRINSCH SQW ($d = 18 \text{ nm}$) structure using TE-polarized light is shown in Fig. 3 for two different absorber biases V_A . Two subbands are clearly identified and are in good agreement with the calculated values. As may be seen, the absorption can be efficiently tuned by varying the bias applied to the absorber. It is worth mentioning that, in general, our MQW structures show well-pronounced exciton peaks in the photocurrent.

The light emission spectrum of a BH GRINSCH SQW laser with a quantum well thickness $d = 14 \text{ nm}$, $L_A = 6 \mu\text{m}$, and $L_C = 800 \mu\text{m}$ is shown in Fig. 4(a) for a gain current $I_G = 250 \text{ mA}$ and an absorber voltage $V_A = +0.3 \text{ V}$. The lasing wavelength under these operating conditions is $\lambda = 1.51 \mu\text{m}$ and TE polarized. Figure 4(b) shows the lasing spectrum for the same structure but a gain current of 330 mA and an absorber voltage $V_A = -0.4 \text{ V}$. As may be seen, the lasing wavelength (also TE polarized) jumped to $\lambda = 1.46 \mu\text{m}$ and a small emission peak remains at $\lambda \sim 1.51 \mu\text{m}$. The average lasing light power that is switched is $\sim 15 \text{ mW}$ per facet and the change in wavelength is $\Delta\lambda = 50 \text{ nm}$. The reason for wavelength switching within the $n = 2$ level is related to the greater available gain at higher photon energies. Thus, with a broadband intracavity absorber (see Fig. 3), quenching of lasing action at longer wavelengths occurs.

It is also worth mentioning that we have observed simi-

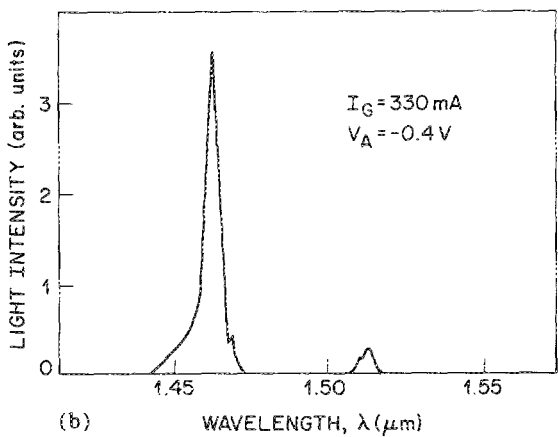
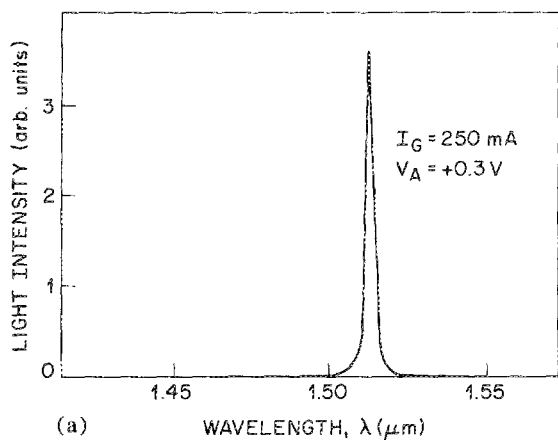


FIG. 4. (a) Light intensity vs wavelength λ , and $I_G = 250$ mA and $V_A = +0.3$ V using a BH GRINSCH SQW laser with $d = 14$ nm, $L_A = 6$ μm , and $L_C = 800$ μm . (b) Light intensity vs wavelength λ and $I_G = 330$ mA and $V_A = -0.4$ V for the same device as in (a).

lar switching characteristics with two QW and four QW structures operating at the $n = 1$ or 2 level. Wavelength switching within the $n = 1$ level with $\lambda \gtrsim 30$ nm is observed when the cavity length of the MQW device is $L_C \gtrsim 400$ μm

and the absorber section length is $L_A \gtrsim 30$ μm . In addition, step-like wavelength switching between the $n = 1$ and 2 levels with $\Delta\lambda \gtrsim 60$ nm is observed when the BH GRINSCH MQW device is cleaved with $L_C \lesssim 300$ μm and $L_A \gtrsim 30$ μm .

In conclusion, we have demonstrated that control of cavity losses combined with the large available gain in InGaAs/InP quantum well lasers can be used to efficiently tune lasing wavelength. By varying voltage applied to an intracavity loss modulator we have achieved discrete, widely separated wavelength switching. While wavelength tuning over a few nm in multielectrode distributed feedback lasers using phase shifting is useful for long distance communication systems⁹ our results showing switching over a few tens of nm's have obvious implications for short haul transmission schemes using wavelength modulation and also various computing, signal processing, and logic applications.

¹C. Shieh, R. Engelmann, J. Mantz, K. Alavi, and C. Shu, *Appl. Phys. Lett.* **54**, 1089 (1989).

²P. S. Zory, A. R. Reisinger, L. J. Mawst, G. Costrini, C. A. Zmudzinski, M. A. Emanuel, M. E. Givens, and I. J. Coleman, *Electron. Lett.* **22**, 475 (1986).

³M. Mittelstein, Y. Arakawa, A. Larson, and A. Yariv, *Appl. Phys. Lett.* **49**, 1689 (1986).

⁴K. Berthold, A. F. J. Levi, S. J. Pearton, R. J. Malik, W. Y. Jan, and J. E. Cunningham, *Appl. Phys. Lett.* **55**, 1382 (1989).

⁵J. Z. Wilcox, S. Ou, J. J. Yang, M. Jansen, and G. L. Peterson, *Appl. Phys. Lett.* **54**, 2174 (1989).

⁶T. Tanbun-Ek, R. A. Logan, H. Temkin, K. Berthold, A. F. J. Levi, and S. N. G. Chu (unpublished); T. Tanbun-Ek, H. Temkin, S. N. G. Chu, and R. A. Logan, *Appl. Phys. Lett.* **55**, 819 (1989).

⁷K. Berthold, A. F. J. Levi, T. Tanbun-Ek, R. A. Logan, and S. N. G. Chu, *Appl. Phys. Lett.* **55**, 1382 (1989).

⁸T. Tanbun-Ek, R. A. Logan, and J. P. Van der Ziel, *Electron. Lett.* **24**, 1483 (1988).

⁹U. Koren, T. L. Koch, B. I. Miller, and A. Shahar, *Appl. Phys. Lett.* **53**, 2132 (1988); T. Numai, S. Murata, and I. Mito, *Appl. Phys. Lett.* **54**, 1859 (1989); and N. K. Dutta, A. B. Piccirilli, T. Cella, and R. L. Brown, *Appl. Phys. Lett.* **48**, 1501 (1986).